



Effects of Radial Imperfection on the Load Capacity of Round Hollow Structural Section Columns

N. Shahbazi^{*a}, S. Tariverdilo^b, A. Amani Dashlekeh^c

^{ab} Faculty of Engineering, Urmia University, Urmia, Iran

^c Faculty of Engineering, University of Mohaghegh Ardabili, Ardabil, Iran

PAPER INFO

Paper history:

Received 13 November 2018

Received in revised form 4 December 2018

Accepted 03 January 2019

Keywords:

Column

Steel Structures

Radial Imperfection

Load Capacity

Buckling

ABSTRACT

Geometric imperfections such as radial imperfection, diamond shape, and local dimples could affect the buckling mode and load carrying capacity of axially compressed steel tubular columns. This paper experimentally investigates the effect of radial imperfection on the load carrying capacity of tubular columns. Test samples include 100 specimens with different values for diameter, length, thickness, imperfection amplitude and imperfection location. Considering applications of columns in buildings, bridges, and offshore jackets, diameter to thickness and slenderness ratios were varied between 20-90 and 17-181, respectively. Results showed that depending on the slenderness ratio and the severity of the imperfection, there was a significant difference between buckling loads of perfect and imperfect specimens.

doi: 10.5829/ije.2019.32.01a.05

NOMENCLATURE

A	Area (mm ²)	LB	Local Buckling (abbreviation)
A_e	Effective area (mm ²)	L_e	Effective length (mm)
A_g	Gross area (mm ²)	P	Axial Load (kgf)
C_c	Critical slenderness (mm/mm)	P_{cr}	Critical load (kgf)
D	Diameter (mm)	P_{eu}	Global critical load, Euler load, $\pi^2 EI/L^2$ (kgf)
E	Elasticity modulus (kgf/cm ²)	P_u	Ultimate axial load (kgf)
e	Eccentricity of axial compression (mm)	Q	Quarter (abbreviation)
e_0	Eccentricity of axial compression in the unloaded state (mm)	R	Radial imperfection location (mm)
EP	Elephant foot (abbreviation)	r	Radius of gyration (mm)
F_a	Allowable stress (kgf/cm ²)	t	Thickness (mm)
F_e	elastic buckling stress (kgf/cm ²)	y_{max}	Maximum distance from cross section neutral axis (mm)
F_y	Yield stress (kgf/cm ²)	Greek Symbols	
GB	Global buckling (abbreviation)	λ	Slenderness ratio (mm/mm)
I	Moment of inertia (mm ⁴)	σ	Stress (kg/cm ²)
IL	Imperfection location (abbreviation)	σ_{cr}	Critical stress (kg/cm ²)
K_{nl}	Correction coefficient	σ_{max}	Maximum stress (kgf/cm ²)
M	Bending moment (kgf/cm)	σ_P, σ_{eP}	Direct stress from compression P at centroid, and stress from flexure due to eccentricity (e) of load P (kgf/cm ²)
ML	Mid height (abbreviation)	σ_u	Ultimate stress (kgf/cm ²)
L	Length (mm)		

*Corresponding Author Email: n_shahbazi@uma.ac.ir (N. Shahbazi)

1. INTRODUCTION

Circular steel columns are widely used in different structures such as bridges, buildings, offshore structures, elevated tanks, oil jackets with different diameter to thickness and slenderness ratios. The problem of buckling behavior of imperfect columns has been an interesting topic for researchers for several decades. The theory of buckling capacity of hollow structural section columns was determined in classic theory (Timoshenko) [1] and Starnes [2] performed an experimental and numerical study on the buckling effect of circular, square and rectangular cutouts in hollow structural section (HSS) columns subject to axial compression.

Geometric imperfection could affect the buckling load of axially loaded steel tubular columns [3, 4]. Researchers have also tried to clarify the interaction between local and global buckling of HSS columns. Chajes [5] reviewed the importance of imperfection in the stability behavior of various types of structural elements [6]. Many surveys on the influence of initial imperfection on the stability of elastic systems were done by Koiter [7]. He clarified the concept of imperfection sensitivity [8].

Krishnakumar and Foster [9] investigated the load carrying capacity of HSS columns with local imperfections. Tafreshi and Colin [10] performed a numerical non-linear finite element study to evaluate the response of composite HSS columns subjected to combined loads, and carried out the post-buckling analysis to investigate the effect of imperfection magnitude on buckling load. Common types of tubular members include square, rectangular and circular hollow sections. Elliptical hollow sections have been recently entered to the construction market. These sections can show better performance than circular hollow sections, especially when the applied bending moment is about the stronger axis or in case of differing lateral load carrying systems in two directions. Some examples of the use of elliptical hollow sections compromise airports at Heathrow in London, UK and Barajas in Madrid, Spain. Previous studies investigated cross-section classification, cross-section design strength in compression and bending about both principal axes and combined shear and bending [11]. Shariati and Mahdizadeh [12] studied the buckling behavior of HSS columns with an elliptical cutout experimentally and numerically. Shu et al. [13] investigated the behavior of cold-formed stainless steel stub columns with square cross section, experimentally and theoretically. Ghanbari, et al. [14] also investigated steel circular tubes with imperfection under axial load experimentally. Guo et al [15] investigated the behavior of thin-walled HSS stub columns under axial compression. Kalantari and Razzaghi [16] implemented a parametric study on vertically stiffened cylindrical shells to investigate the buckling capacity using ANSYS

software. Rastgar and Showkati [17] monitored the construction of steel cylindrical tanks in one of the refinery site using a field survey and introduced the created imperfections. Most of these studies have investigated the imperfection effect on short columns with low slenderness and with limited number of samples, which cannot represent the behavior of structures and buildings' columns.

This paper presents an experimental study on 100 specimens included radial geometric imperfection with 5 diameters (50.8, 38.1, 25.4, 20 and 13 mm), two magnitudes of imperfection (D/8 and D/4), different locations for imperfection (Mid-height and Quarter-height) and different slenderness ratios (17 to 181) and investigates the interaction between these imperfections and the columns load carrying capacity.

2. LOAD CARRYING CAPACITY OF TUBULAR COLUMNS

Load carrying capacity of tubular columns is controlled by interaction between its local and global buckling modes. This section reviews AISC 360 [18] requirement regarding global and local buckling of steel tubular columns.

The Euler elastic buckling load of columns is given by following equation:

$$P_{cr} = \frac{\pi^2 EI}{(L_e)^2} \quad (1)$$

Considering $\lambda = \frac{L_e}{r}$ and $r = \sqrt{\frac{I}{A}}$, the corresponding stress will be

$$F_e = \frac{P_{cr}}{A} = \frac{\pi^2 E}{(\lambda)^2} \quad (2)$$

This elastic buckling load is only applicable to slender column. Considering the effect of residual stresses, AISC 360 [18] accounts for elasto-plastic buckling for columns with critical stress carrying capacity as follows:

- For slender columns with $\lambda > 4.71 \sqrt{\frac{E}{F_y}}$ or $F_e < 0.44F_y$

$$\sigma_{cr} = 0.877F_e \quad (3a)$$

- For short columns with $\lambda \leq 4.71 \sqrt{\frac{E}{F_y}}$ or $F_e \geq 0.44F_y$

$$\sigma_{cr} = \left[0.658 \frac{F_y}{F_e} \right] F_y \quad (3b)$$

Most of building columns could be categorized as short columns that experience inelastic buckling [19, 20].

According to AISC 360 [18], D/t or b/t ratios should be controlled in tubular sections. The effective section area (A_e) in circular hollow sections with slender elements is calculated based on D/t ratio as follows:

- For $\frac{D}{t} < 0.11 \frac{E}{F_y}$

$$A_e = A_g \quad (4a)$$

$$\text{- For } 0.11 \frac{E}{F_y} < \frac{D}{t} < 0.45 \frac{E}{F_y}$$

$$A_e = \left[\frac{0.038E}{F_y(D/t)} + \frac{2}{3} \right] A_g \quad (4b)$$

For ST37 steel local buckling happens when D/t ratio is greater than $96.25 (= 0.11 \frac{E}{F_y})$. Considering practical applications and to remove the possibility of local buckling, in this study D/t ratio is taken smaller than 96.25 [21].

3. EFFECT OF IMPERFECTIONS ON THE LOAD CARRYING CAPACITY

Geometric imperfection causes eccentricity in the cross section. Eccentricity could give rise to perturbation in the stress pattern and cause a local increase in stress [22]. While axial tension reduces the possibility of formation of plastic hinging, axial compression steeply amplifies the perturbation in stress pattern and results in the formation of plastic hinge and failure of the column and decrease in column's load carrying capacity [20].

Amplification of eccentricity due to axial compression could be formulated as follows:

$$e = e_0 K_{nl} \quad (5)$$

$$K_{nl} = 1/(1 - P/P_{eu}) = P_{eu}/(P_{eu} - P) \quad (6)$$

The eccentricity e of the compressive load P in a cross section increases the maximum stress from uniform compressive stress σ_p to σ_{max}

$$\sigma_{max} = \sigma_p + \sigma_{ep} \quad (7)$$

$$\sigma_p = P/A \quad (8)$$

$$\sigma_{ep} = Pe y_{max}/I \quad (9)$$

where y_{max} is the maximum distance on the section from its neutral axis, and I represents section's moment of inertia. The stress increase σ_{ep} could be significant in a slender column even if the initial imperfection e_0 is minor relative to the column length [23, 24].

In order to quantitatively capture the geometric interaction of local and global failure in design, one should limit the maximum stress in Equation (7), evaluated in the context of the nonlinearly amplified eccentricity, and in Equations (5) and (6), to the local critical threshold [24-26].

4. EXPERIMENTAL PROGRAM

An experimental study was conducted in order to evaluate the effect of radial geometric imperfection on

the load carrying capacity of tubular columns with different slenderness ratios and severities and locations of imperfection. The experimental setup is shown in Figure 1. The load was statically applied to the specimens with a hydraulic jack to 50000 kg with a loading rate of 2 mm/min as axial load. A linear variable differential transformers (LVDT) was placed at the end of the column to measure the axial displacement. The simply and pinned supports were used in two ends of specimens as shown in Figure 1.

HSS columns are widely used in tall buildings due to their aesthetic appearance. They are also used in parking buildings, bridges, offshore oil jackets, piers, air tanks, industrial buildings and etc. Tubular columns are known as economic sections because of their section properties (less material and better performance). So it is important to evaluate their buckling behavior. Different types of imperfection that can occur in tubular sections or thin-walled cylindrical shells include mechanical and geometric imperfections. Mechanical imperfections include residual stress, load eccentricity and lack of fit. Geometric imperfections, which is the goal of the current study, include initial bowing, radial imperfection, crack and diamond shape imperfections. Bjornsson [27] studied the initial imperfection effect on columns behavior with solving some examples.

Radial imperfection, which is studied in this paper, usually occurs as a result of impact and sometimes accompanies a hole. Radial imperfection causes a reduction in the moment of inertia and increases the eccentricity and consequently results in a decrease in load carrying capacity of the column by helping plastic hinge formation in the imperfection location. Steel balls with different diameters and a vise were used to impose imperfection with different amplitudes in experimental procedure.

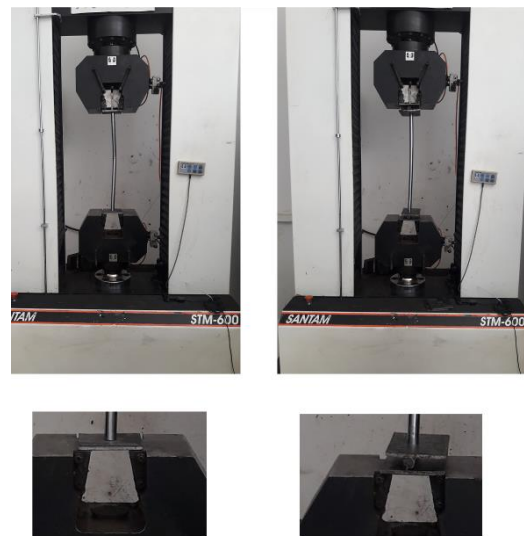


Figure 1. Experimental setup

Also to control the amplitude of imperfection, a caliper was used as shown in Figure 2.

Experimental specimens should reflect properties of real columns. Therefore, 100 specimens were tested in this study with different heights (300, 400, 600, 800 mm), different severities of imperfection ($D/8$, $D/4$), different locations of imperfection (Mid-height and Quarter-height) and different diameters (50.8, 38.1, 25.4, 20, 13 mm) as shown in Figures 3 and 4. Properties of the specimens and experimental results are shown in Table 1.

5. RESULTS AND DISCUSSION

Different types of failure of HSS column include elephant foot failure, local buckling with elephant foot failure and local buckling with global buckling. Elephant foot failure occurs without buckling in columns with low slenderness. Elephant foot is actually a local failure in the support (Figure 5). According to Shariati et al. [12] and Ghanbari et al. [14], short columns (low slenderness) fail with elephant foot mode and imperfection is not detrimental on the compression member behavior. Results of these studies were in line with our results, but their specimen sizes did not cover common sizes for structural elements. Unfortunately, studies on slender columns has been very limited.



Figure 2. Tools used to impose imperfection



Figure 3. Specimens with different diameters and equal lengths

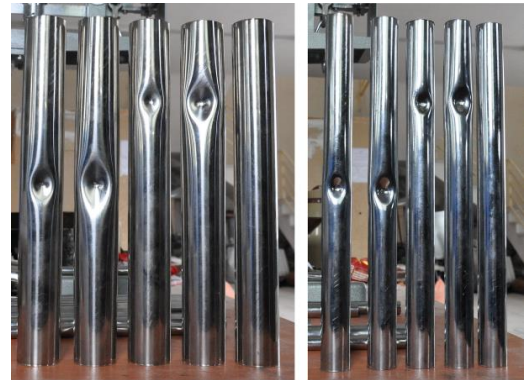


Figure 4. Specimens with different imperfections and diameters

Local buckling with elephant foot failure occurs in columns with medium slenderness. This failure starts with local buckling in the imperfection location (diamond shape failure) and then is accompanied by elephant foot failure mode (Figure 6).

Local buckling with global buckling occurs in slender columns which are more prone to buckle. Depending on the amplitude of imperfection, local buckling can occur in the middle or quarter height (imperfection location) and results in global buckling (Figures 7 and 8).

Due to use of simple space frame plus bracing as the structural system in the most of common buildings (continuous columns and pinned connection of beams), it is predicted that simply support condition can result in realistic results. The load carrying capacity and failure types of samples with simply and pinned supports were tested and compared. Significant differences did not observe in the results. For example, elephant foot failure observed in both simply and pinned supported specimens with 50.8 mm diameter and 600 mm length ($\lambda=33.78$). Local buckling and elephant foot failure occurred in both simply and pinned supported specimens with 38.1 mm diameter and 600 mm length ($\lambda=45.21$). Also, both simply and pinned supported specimens with 20 mm diameter and 600 mm length ($\lambda=88.23$) failed due to local and global buckling.

According to the experimental results of 100 HSS columns with 5 different diameters, heights and imperfections, and based on their behavior and failure modes, they can be classified in three groups:

- Tubes with low slenderness ($\lambda < 33.78$); Failure starts at one end of the column and continues with elephant foot mode until the columns load carrying capacity ceases. The decrease in load carrying capacity is not significant in this state (EP) (Figure 5).

- Tubes with slenderness ratios more than 33.78 and less than 60.29; failure starts in the imperfection location and continues with local hardening (Diamond shape).

TABLE 1. Properties and configuration of tested specimens

Sample	D(mm)	t(mm)	D/t	L(mm)	λ	R(mm)	IL	P_u (kg)	σ_u (kg/cm ²)	Failure Mode
1	50.8	0.57	89	300	17	0	-	3210	3567	EP
2	50.8	0.57	89	300	17	D/8	M	3060	3400	EP
3	50.8	0.57	89	300	17	D/8	Q	3150	3500	EP
4	50.8	0.57	89	300	17	D/4	M	2860	3178	EP
5	50.8	0.57	89	300	17	D/4	Q	2970	3300	EP
6	50.8	0.57	89	400	22.5	0	-	3100	3444	EP
7	50.8	0.57	89	400	22.5	D/8	M	2820	3133	EP
8	50.8	0.57	89	400	22.5	D/8	Q	2890	3211	EP
9	50.8	0.57	89	400	22.5	D/4	M	2630	2922	EP
10	50.8	0.57	89	400	22.5	D/4	Q	2730	3033	EP
11	50.8	0.57	89	600	33.78	0	-	2980	3311	EP
12	50.8	0.57	89	600	33.78	D/8	M	2850	3167	EP
13	50.8	0.57	89	600	33.78	D/8	Q	3110	3456	EP
14	50.8	0.57	89	600	33.78	D/4	M	2650	2944	EP
15	50.8	0.57	89	600	33.78	D/4	Q	2750	3056	EP
16	50.8	0.57	89	800	45	0	-	2770	3078	EP+LB
17	50.8	0.57	89	800	45	D/8	M	2150	2389	EP+LB
18	50.8	0.57	89	800	45	D/8	Q	2250	2500	EP+LB
19	50.8	0.57	89	800	45	D/4	M	1600	1778	EP+LB
20	50.8	0.57	89	800	45	D/4	Q	1990	2211	EP+LB
21	38.1	0.57	66.8	300	22.61	0	-	2320	3463	EP
22	38.1	0.57	66.8	300	22.61	D/8	M	2210	3298	EP
23	38.1	0.57	66.8	300	22.61	D/8	Q	2280	3403	EP
24	38.1	0.57	66.8	300	22.61	D/4	M	2060	3075	EP
25	38.1	0.57	66.8	300	22.61	D/4	Q	2150	3209	EP
26	38.1	0.57	66.8	400	30.14	0	-	2250	3358	EP
27	38.1	0.57	66.8	400	30.14	D/8	M	2150	3209	EP
28	38.1	0.57	66.8	400	30.14	D/8	Q	2200	3283	EP
29	38.1	0.57	66.8	400	30.14	D/4	M	2000	2985	EP
30	38.1	0.57	66.8	400	30.14	D/4	Q	2090	3119	EP
31	38.1	0.57	66.8	600	45.21	0	-	2080	3104	EP+LB
32	38.1	0.57	66.8	600	45.21	D/8	M	1630	2433	EP+LB
33	38.1	0.57	66.8	600	45.21	D/8	Q	1680	2507	EP+LB
34	38.1	0.57	66.8	600	45.21	D/4	M	1270	1895	EP+LB
35	38.1	0.57	66.8	600	45.21	D/4	Q	1500	2239	EP+LB
36	38.1	0.57	66.8	800	60.29	0	-	1960	2925	LB+GB
37	38.1	0.57	66.8	800	60.29	D/8	M	1530	2283	LB+GB
38	38.1	0.57	66.8	800	60.29	D/8	Q	1590	2373	LB+GB
39	38.1	0.57	66.8	800	60.29	D/4	M	1270	1895	LB+GB
40	38.1	0.57	66.8	800	60.29	D/4	Q	1410	2104	LB+GB
41	25.4	0.59	44.56	300	34.17	0	-	1510	3283	EP
42	25.4	0.59	44.56	300	34.17	D/8	M	1330	2891	EP
43	25.4	0.59	44.56	300	34.17	D/8	Q	1470	3196	EP
44	25.4	0.59	44.56	300	34.17	D/4	M	1330	2891	EP
45	25.4	0.59	44.56	300	34.17	D/4	Q	1390	3022	EP
46	25.4	0.59	44.56	400	45.56	0	-	1410	3065	EP+LB
47	25.4	0.59	44.56	400	45.56	D/8	M	1090	2369	EP+LB
48	25.4	0.59	44.56	400	45.56	D/8	Q	1140	2478	EP+LB
49	25.4	0.59	44.56	400	45.56	D/4	M	910	1978	EP+LB
50	25.4	0.59	44.56	400	45.56	D/4	Q	1010	2196	EP+LB
51	25.4	0.59	44.56	600	68.34	0	-	1210	2630	LB+GB
52	25.4	0.59	44.56	600	68.34	D/8	M	930	2022	LB+GB
53	25.4	0.59	44.56	600	68.34	D/8	Q	980	2130	LB+GB
54	25.4	0.59	44.56	600	68.34	D/4	M	790	1717	LB+GB
55	25.4	0.59	44.56	600	68.34	D/4	Q	930	2022	LB+GB
56	25.4	0.59	44.56	800	91.12	0	-	900	1956	LB+GB
57	25.4	0.59	44.56	800	91.12	D/8	M	700	1522	LB+GB
58	25.4	0.59	44.56	800	91.12	D/8	Q	730	1587	LB+GB
59	25.4	0.59	44.56	800	91.12	D/4	M	590	1283	LB+GB

TABLE 1. Continue- Properties and configuration of tested specimens

Sample	D(mm)	t(mm)	D/t	L(mm)	λ	R(mm)	IL	P_u (kg)	σ_u (kg/cm ²)	Failure Mode
60	25.4	0.59	44.56	800	91.12	D/4	Q	810	1761	LB+GB
61	20	0.68	29.4	300	44.12	0	-	1260	3051	EP+LB
62	20	0.68	29.4	300	44.12	D/8	M	980	2373	EP+LB
63	20	0.68	29.4	300	44.12	D/8	Q	1010	2445	EP+LB
64	20	0.68	29.4	300	44.12	D/4	M	820	1985	EP+LB
65	20	0.68	29.4	300	44.12	D/4	Q	900	2179	EP+LB
66	20	0.68	29.4	400	58.82	0	-	1230	2978	LB+GB
67	20	0.68	29.4	400	58.82	D/8	M	840	2034	LB+GB
68	20	0.68	29.4	400	58.82	D/8	Q	880	2131	LB+GB
69	20	0.68	29.4	400	58.82	D/4	M	710	1719	LB+GB
70	20	0.68	29.4	400	58.82	D/4	Q	770	1864	LB+GB
71	20	0.68	29.4	600	88.23	0	-	890	2155	LB+GB
72	20	0.68	29.4	600	88.23	D/8	M	690	1671	LB+GB
73	20	0.68	29.4	600	88.23	D/8	Q	720	1743	LB+GB
74	20	0.68	29.4	600	88.23	D/4	M	570	1380	LB+GB
75	20	0.68	29.4	600	88.23	D/4	Q	640	1550	LB+GB
76	20	0.68	29.4	800	117.65	0	-	570	1380	LB+GB
77	20	0.68	29.4	800	117.65	D/8	M	450	1089	LB+GB
78	20	0.68	29.4	800	117.65	D/8	Q	430	1041	LB+GB
79	20	0.68	29.4	800	117.65	D/4	M	370	896	LB+GB
80	20	0.68	29.4	800	117.65	D/4	Q	410	993	LB+GB
81	13	0.51	25.5	300	67.87	0	-	530	2650	LB+GB
82	13	0.51	25.5	300	67.87	D/8	M	420	2100	LB+GB
83	13	0.51	25.5	300	67.87	D/8	Q	540	2700	LB+GB
84	13	0.51	25.5	300	67.87	D/4	M	340	1700	LB+GB
85	13	0.51	25.5	300	67.87	D/4	Q	390	1950	LB+GB
86	13	0.51	25.5	400	90.5	0	-	400	2000	LB+GB
87	13	0.51	25.5	400	90.5	D/8	M	310	1550	LB+GB
88	13	0.51	25.5	400	90.5	D/8	Q	330	1650	LB+GB
89	13	0.51	25.5	400	90.5	D/4	M	260	1300	LB+GB
90	13	0.51	25.5	400	90.5	D/4	Q	290	1450	LB+GB
91	13	0.51	25.5	600	135.75	0	-	220	1100	LB+GB
92	13	0.51	25.5	600	135.75	D/8	M	170	850	LB+GB
93	13	0.51	25.5	600	135.75	D/8	Q	170	850	LB+GB
94	13	0.51	25.5	600	135.75	D/4	M	140	700	LB+GB
95	13	0.51	25.5	600	135.75	D/4	Q	160	800	LB+GB
96	13	0.51	25.5	800	181	0	-	130	650	LB+GB
97	13	0.51	25.5	800	181	D/8	M	90	450	LB+GB
98	13	0.51	25.5	800	181	D/8	Q	100	500	LB+GB
99	13	0.51	25.5	800	181	D/4	M	80	400	LB+GB
100	13	0.51	25.5	800	181	D/4	Q	90	450	LB+GB



Figure 5. Elephant foot failure



Figure 6. Diamond shape failure



Figure 7. Buckling in mid height



Figure 8. Buckling in quarter height

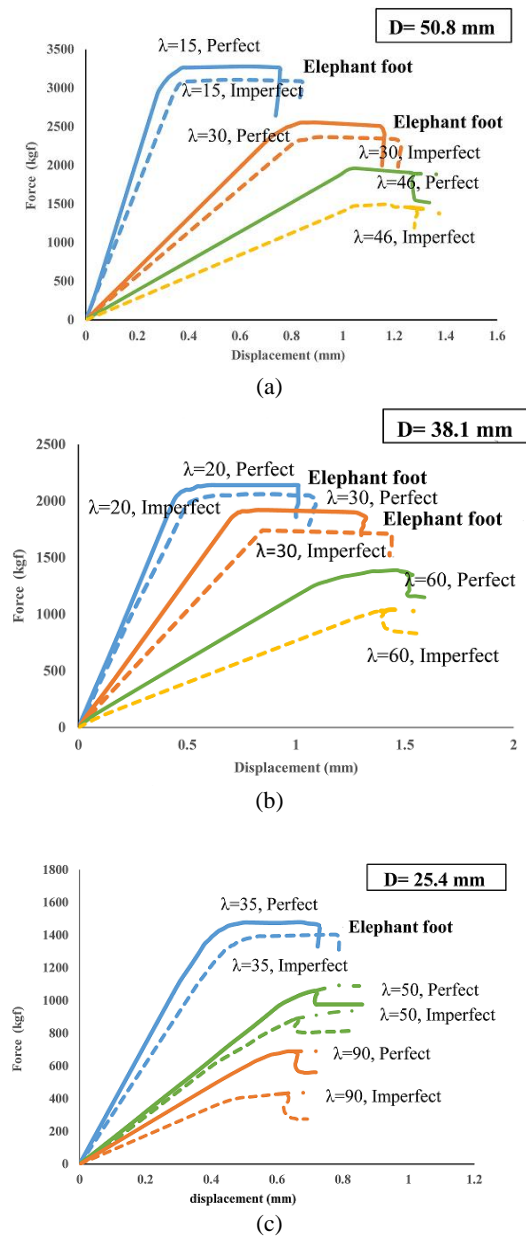
In comparison with the former class, the decrease in load carrying capacity of imperfect column is more noticeable (EP+LB) (Figure 6).

-Tubes with slenderness ratios greater than 60.29; Failure starts with forming of the plastic hinge in the imperfection location and continues with global buckling. In these columns the decrease of load carrying capacity is significant (LB+GB) (Figures 7 and 8).

Force-displacement curves of the specimens with different diameters and slenderness ratios are shown in Figure 9. According to Figures 9a and 9b, for tubes with large diameters ($D=50.8, 38.1$ mm) and low slenderness and L/D ratios, deformation under the load is predominated by elephant foot failure at the end of column. In case of a severe imperfection, both elephant foot failure at the end and local buckling at the imperfect point will occur. Generally, imperfection does not have a significant influence on the load carrying capacity of these columns. By increasing the slenderness (λ), the section will show a different behavior, in which failure starts with local buckling in the imperfection location and continues with development of plastic hinge in that point and finishes with bifurcation. According to Figure 9c, for tubes with medium diameter ($D=25.4$ mm) and low slenderness and L/D ratios, deformation under the load is predominated by elephant foot failure at the end of column and imperfection does not have a significant influence. By increasing the slenderness ($\lambda > 40$) failure starts with local buckling in the imperfection location and continues with the development of plastic hinge in this point and finally finishes with bifurcation. According to Figures 9d and 9e, for tubes with small diameters ($D=20$ or 13 mm), imperfection is detrimental and elephant foot

failure will not occur. Section fails with local buckling in the imperfection location which continues with plastic hinge development in the imperfection point and bifurcation.

Considering elephant foot failure in very short columns and elephant foot and local buckling failure in short columns, the decrease in their load carrying capacity is smaller than slender columns with local and global buckling. So, in a general classification, all columns can be classified in two groups as columns with slenderness ratio less than 40 and greater than 40. The imperfection severity effect on load carrying capacity of columns for different locations of imperfection is shown in Figure 10.



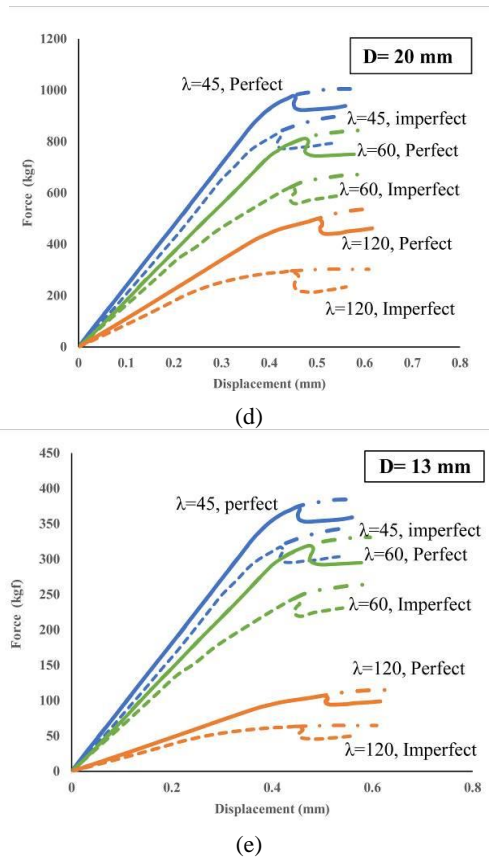


Figure 9. Force-Displacement curves of the specimens with different diameter and slenderness

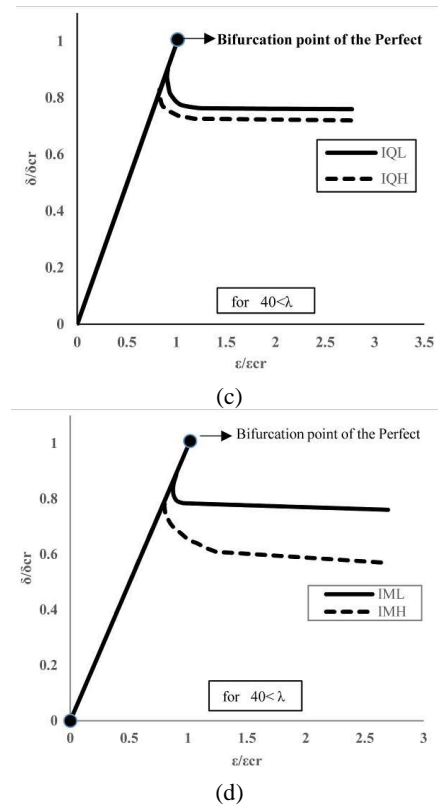
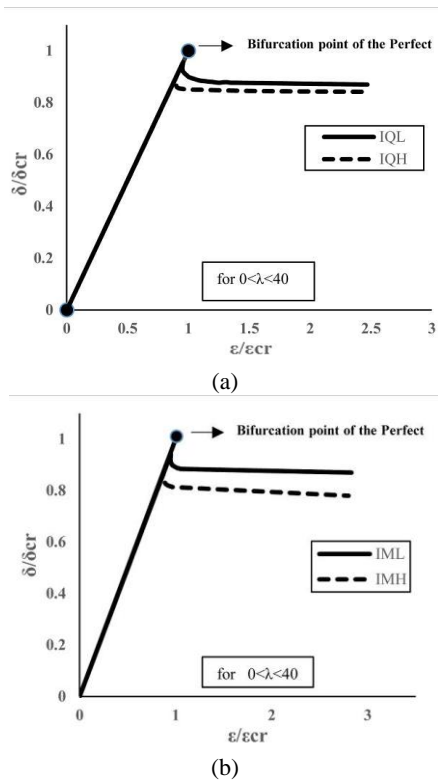


Figure 10. Effect of slenderness and imperfection on the load carrying capacity

The results of this study have been shown in Figure 11, which aligns with the results of Somodi's study [28] on flexural buckling resistance of high strength steel square columns. It is clear that the results of perfect specimens have good agreement with AISC360 [18].

Considering experimental samples (100 samples) including perfect (P), severe imperfection in mid-height (IMH), low imperfection in mid-height (IML), severe imperfection in quarter-height (IQH) and low imperfection in quarter-height (IQL) in which low

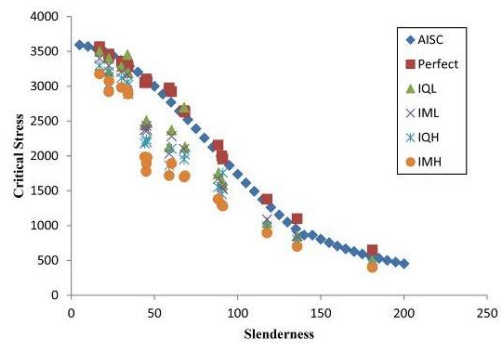


Figure 11. Slenderness-Critical stress curves for experimental specimens and AISC

imperfection equals $D/8$ and sever imperfection equals $D/4$, the following graph shown in Figure 12 can be obtained.

For specimens with $17 < \lambda < 181$, load carrying capacity decrease are 7-20%, 12-25%, 15-30% and 22-45% for IQL, IML, IQH and IMH in comparison with the perfect specimens.

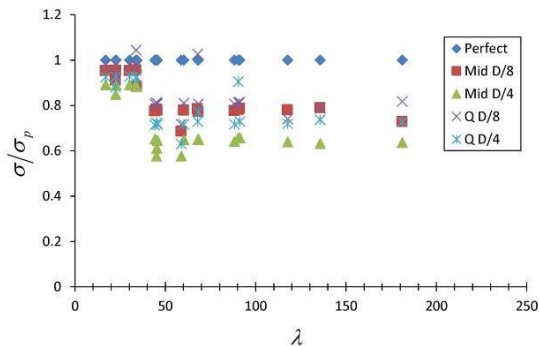


Figure 12. Slenderness and imperfection relation

6. CONCLUSION

According to the above results, column behavior in respect of imperfection influence can be classified in three groups:

- Very short columns: in which slenderness is less than 35 ($\lambda < 35$), imperfection has a slight influence in decreasing the compression member's load carrying capacity. Plastic hinge develops in one end or in imperfection location. The percentage of decrease in load carrying capacity is about 5-15%.

- Short columns: in which slenderness is in the range of 35-60 ($35 < \lambda < 60$). These columns have an elastic-plastic behavior under compression. Plastic hinge develops in imperfection location. The percentage of decrease in load carrying capacity is about 10-20%.

- Slender columns: in which slenderness is greater than 60 ($60 < \lambda < 180$). In these columns buckling occurs in the imperfection location and leads to column's failure. The percentage of decrease in load carrying capacity in these columns is significant and is about 15-45%.

It should be noted that imposing the imperfection on the column cannot be very accurate, so there will be a slight difference between theoretic and experimental values.

7. REFERENCES

1. Timoshenko S.P., Gere J.M., "Theory of elastic stability", 2nd ed. Singapore, McGraw-Hill, (1965).
2. Starnes, Jr. J. H., "The effects of cutouts on the buckling of thin shells", *Thin-shell structures*, Prentice-Hall, (1974), 289-304.

3. Horton, W.H. and Durham, S.C., "Imperfections, a main contributor to scatter in experimental values of buckling load", *International Journal of Solids and Structures*, Vol. 1, No. 1, (1965), 59-62, IN1-IN2, 63-70, IN3, 71-72.
4. Koiter, W.T., "The effect of axisymmetric imperfection on the buckling of cylindrical shells under axial compression", *Academia van Wetenschappen-Amsterdam*, Series B, No. 66, (1963), 265-279.
5. Chajes, A., "Post-buckling Behavior", *Journal of Structural Engineering*, 109, (1983), 2450-2462.
6. Nishimori, F. "Influential mode of imperfection on carrying capacity of structures", *Journal of Engineering Mechanics*, Vol. 115, (1989), 2150-2165.
7. Koiter, W.T., "About the stability of the elastic balance (in Dutch)", Thesis Delft, Amsterdam, (1945).
8. Hutchinson, J. W. and Koiter, W. T., "Postbuckling theory", *Applied Mechanics*, Rev. 23, (1970), 1353-1366.
9. Krishnakumar, S. and Foster, C.G., "Axial load capacity of cylindrical shells with local geometric defects", *Experimental Mechanics*, (1991), 104-110.
10. Tafreshi, A., and Colin, G.B., "Instability of imperfect composite cylindrical shells under combined loading", *Composite Structures*, Vol.80, No. 1, (2006), 49-64.
11. Chan, T. M., and Gardner, L., "Flexural buckling of elliptical hollow section columns", *Journal of Structural Engineering*, (2009), 546-557.
12. Shariati, M., and Mahdizadeh Rokhi, M., "Buckling of steel cylindrical shells with an elliptical cutout", *International Journal of Steel Structures*, Vol. 10, No. 2, (2010), 193-205.
13. Shu, G., Zheng, B., and Shen, X., "Experimental and theoretical study on the behavior of cold-formed stainless steel stub columns", *International Journal of Steel Structures*, Vol. 13, No. 1, (2013), 141-153.
14. Ghanbari Ghazijahani, T., Jiao, H., and Holloway, D., "Plastic buckling of dented steel circular tubes under axial compression: An experimental study", *Thin-Walled Structures*, Vol. 92, (2015), 48-54.
15. Guo, L., Liu, Y., Jiao, H., and An, S. "Behavior of thin-walled circular hollow section stub columns under axial compression", *International Journal of Steel Structures*, Vol. 16, No. 3, (2016), 777-787.
16. Kalantari, Z., and Razzaghi, M. S., "Predicting the buckling Capacity of Steel Cylindrical Shells with Rectangular Stringers under Axial Loading by using Artificial Neural Networks", *International Journal of Engineering (IJE), Transactions B: Applications*, Vol. 28, No. 8, (2015), 1154-1159.
17. Rastgar, M., and Showkati, H., "Field Study and Evaluation of Buckling Behavior of Cylindrical Steel Tanks with Geometric Imperfections under Uniform External Pressure", *International Journal of Engineering, Transactions C: Aspects*, Vol. 30, No. 9, (2017), 1309-1318.
18. "Specification for structural steel buildings", American Institute of Steel Construction, Chicago: ANSI/AISC 360-16, (2016).
19. Salmon, C.G., Johnson, J.E., and Malhas, F.A., "Steel structures design and behavior", Prentice-Hall, (2009).
20. Greschik, G., "Global imperfection-based column stability analysis", 48th structures, structural dynamics, and materials conference, April 23-26, (2007).
21. Gavrilenko, G.D., "Stability of cylindrical shells with local imperfections", *International Applied Mechanics*, Vol. 38, No. 12, (2002), 1496-1500.
22. Schneider, W. "Stimulating equivalent geometrical imperfections for the numerical buckling strength verification of axially

- compressed cylindrical steel shells”, *Computational Mechanics*, Vol. 37, No. 3, (2006), 530–536.
23. Teng, J.G., and Rotter, J.M., “Buckling of pressurized axisymmetrically imperfect cylinders under axial loads”, *Journal of Engineering Mechanics*, Vol. 118, (1992), 229-247.
 24. Wullschleger, L., and Piening Meyer, H.R., “Buckling of geometrically imperfect cylindrical shells-definition of a buckling load”, *International Journal of Non- Linear Mechanics*, (2002), 645–57.
 25. Gavrilenko, G.D., and Krasovski, V.L., “Stability of circular cylindrical shells with a single local dent”, *Strength of Materials*, Vol. 36, No. 3, (2004), 260–268.
 26. Jiao, H., and Zhao, X.L., “Imperfection, residual Stress and yield slenderness of very high strength (VHS) circular steel tubes”, *Journal of Constructional Steel Research*, Vol. 59, (2003), 233-249.
 27. Bjornsson, T., “Structural analysis of columns with initial imperfections”, M.Sc. thesis, Faculty of Civil and Environmental Engineering, University of Iceland, (2017).
 28. Somodi, B., “Flexural buckling resistance of high strength steel welded and cold-formed square closed section columns”, Thesis of dissertation, Faculty of Civil Engineering, Budapest University of Technology and Economics, (2017).

Effects of Radial Imperfection on the Load Capacity of Round Hollow Structural Section Columns

N. Shahbazi^a, S. Tariverdilo^b, A. Amani Dashlejh^c

^{a,b} Faculty of Engineering, Urmia University, Urmia, Iran

^c Faculty of Engineering, University of Mohaghegh Ardabili, Ardabil, Iran

P A P E R I N F O

چکیده

Paper history:

Received 13 November 2018

Received in revised form 4 December 2018

Accepted 04 January 2019

Keywords:

Column

Steel Structures

Radial Imperfection

Load Capacity

Buckling

ناکاملی‌های هندسی همچون ناکاملی شعاعی، الماسی شکل و گودافتادگی موضعی می‌توانند بر مود کمانش و ظرفیت باربری ستونهای جدارنازک تحت بارهای فشاری محوری تاثیرگذار باشند. این مقاله اثر ناکاملی شعاعی بر ظرفیت باربری ستونهای جدارنازک را به طور آزمایشگاهی مورد بررسی قرار می‌دهد. با توجه به کاربرد ستونها در ساختمانها، پلها و سازه‌های دریایی، نسبت قطر به ضخامت و لاغری به ترتیب بین ۲۰ تا ۹۰ و ۱۷ تا ۱۸۱ در نظر گرفته شده است. نتایج نشان می‌دهد که بسته به نسبت لاغری و شدت ناکاملی، تفاوت عمده‌ای بین ظرفیت کمانشی ستونهای کامل و ناکامل وجود دارد.

doi: 10.5829/ije.2019.32.01a.05